

Article

A Promising Process to Remove Nitrate from Solar Panel Production Wastewater and Meanwhile Generating Electricity

Libin Chen ¹, Cong Ding ², Bingyin Liu ², Jinshi Lian ², Lingling Lai ², Linjiang Yuan ² and Ru Wang ^{2,*}

¹ Shaanxi Provincial Land Engineering Construction Group Co., Ltd., Xi'an 710075, China; chenlb_047300@163.com

² Department of Environmental Engineering, Xi'an University of Architecture and Technology, Xi'an 710055, China; dc1210673668@163.com (C.D.); liudoudou0117@163.com (B.L.); lianjinshi@xauat.edu.cn (J.L.); yu_183@163.com (L.L.); yuanlinjiang@xauat.edu.cn (L.Y.)

* Correspondence: wangru890501@163.com

Abstract: For traditional heterotrophic denitrification technology, organics are usually added as the electron donor for nitrate removal, which increases the operation cost for wastewater treatment. Solar panel production wastewater contains a large amount of nitrate. To decrease the operation cost and reduce CO₂ emissions, an iron anode microbial fuel cell (Fe-MFC) was constructed to treat solar panel production wastewater by sequencing batch operation. The results showed that the maximum nitrate removal efficiency reached 99.98% and the maximum removal rate was 0.049 kg·m⁻³·d⁻¹. The output voltages rose rapidly to 560 ± 10 mV within 2 h and then stabilized at 520 ± 50 mV for about 40 h. Combining the detection of coulombic efficiency, CV curve, q* value and internal resistance; the decrease in denitrification efficiency and electricity generation efficiency probably resulted from the passivation of iron anode and the aging of the cathode biofilm resulted in the efficiency decrease. From the microbial analysis, *Chryseobacterium*, *Thermomonas* and *Thauera* predominated at the end of Fe-MFC operation. Microorganisms that cannot adapt to the autotrophic environment in Fe-MFC died out finally. Periodic replacement of the iron anode and domestication of the bio-cathode were essential to maintain the Fe-MFC efficiency. The Fe-MFC technology was feasible to be used to remove nitrate and generate electricity from solar panel production wastewater. Without organics addition, the Fe-MFC technology was cost-efficient and environmentally friendly, endowing itself with a broad prospect of application.

Keywords: sheet iron; microbial fuel cell; denitrification; electricity generation



Citation: Chen, L.; Ding, C.; Liu, B.; Lian, J.; Lai, L.; Yuan, L.; Wang, R. A Promising Process to Remove Nitrate from Solar Panel Production Wastewater and Meanwhile Generating Electricity. *Water* **2023**, *15*, 3347. <https://doi.org/10.3390/w15193347>

Academic Editor:
Alejandro Gonzalez-Martinez

Received: 7 August 2023
Revised: 18 September 2023
Accepted: 20 September 2023
Published: 24 September 2023



Copyright: © 2023 by the authors. Licensee MDPI, Basel, Switzerland. This article is an open access article distributed under the terms and conditions of the Creative Commons Attribution (CC BY) license (<https://creativecommons.org/licenses/by/4.0/>).

1. Introduction

The emission of nitrogen compounds by human activities has exceeded the environmental capacity thus forming a certain threat to the ecology [1]. People believe that the environmental and ecological problems caused by nitrogen pollution will be more serious than global warming [2]. Aquatic nitrogen pollution may cause eutrophication and other potential harm to the natural environment and human health [3,4].

Nitrate (NO₃⁻) is one of the most stable forms of nitrogen-containing compounds in aerobic environments [5–7], its concentration in polluted wastewater could not be underestimated up till now. Relevant studies show that industrial effluents account for the largest proportion of nitrogen pollution [7–9]. Photovoltaic industrial parks produce a large amount of solar panel production wastewater per day, with a high NO₃⁻ concentration [10]. It is of great significance to remove the NO₃⁻ pollutants from solar panel production wastewater [11].

Physical and chemical technologies have been applied to treat nitrogen pollution in wastewater, such as air stripping and reverse osmosis [12], but these technologies may produce nitrite (NO₂⁻), nitrous oxide (N₂O) and other secondary pollutants, causing inconvenience to the subsequent treatment [13–15]. The end-product of biological nitrogen

removal technology is N_2 , which is environmentally friendly. As for NO_3^- removal from the solar panel production wastewater, the most widely method was also the multiple combinations of biochemical techniques [16]. Thus, the biological removal of NO_3^- draws more and more attention.

Organics were usually used as the electron donor for denitrification. However, for most industrial wastewaters, organics were deficient. Glucose, methanol and acetate were commonly purchased and added to the wastewater as the electron donor for denitrification [6,15,17]. To save costs and decrease the emission of carbon dioxide, biological autotrophic denitrification technology, especially with the cathode as an electron donor came into people's vision [18].

Bio-cathode denitrification is one of the most popular biological technologies for nitrogen removal in recent years [19]. Bio-cathode in MFC directly provides electrons for denitrification [20]. Clauwaert et al. constructed the first bio-cathode denitrification MFC in the world, with bio-anode organics oxidation [21]. Wu et al. successfully used a one-chamber MFC reactor to treat coking wastewater, achieving the simultaneous removal of nitrogen and organics [22]. Meanwhile, bio-cathode MFC combined with aerobic nitrification could increase the nitrate removal efficiency and electricity production capacity [23]. When MFC was combined with the A/A/O wastewater treatment process to construct the MFC-A/A/O reactor, the removal rate of organics and nitrogen increased by 15.93% and 9.25% on average, and the output voltage reached 168.8 ± 8.2 mV [24,25]. In the bio-cathode denitrification MFC system, denitrifying microorganisms were cultured to form a biofilm on the cathode, and the biofilm performed nitrate reduction activity [26]. The bio-cathode denitrification MFC technology showed impressive treatment efficiencies for NO_3^- -containing wastewater.

Compared with the bio-anode, the iron anode would be a better choice for denitrification MFC system, as (1) the iron anode has strong electron donor potential and (2) iron is cheap and quite available [1,20,27]. Iron anodes have been used by Li et al. to provide electrons for a bio-cathode, which removed nitrate from wastewater economically and environmentally friendly [28].

To develop a cost-effective nitrate removal technology treating solar panel production wastewater, a two-chamber MFC was adopted with sheet iron as the anode. Denitrification biofilm was cultured on the carbon brush as the bio-cathode. Then, an iron anode and bio-cathode microbial fuel cell (Fe-MFC) was established to treat solar panel production wastewater. The nitrate removal efficiency and the electricity generation efficiency were determined, and the microbial morphology and community were analyzed. Based on the results, the mechanism of nitrate removal on bio-cathode was revealed, and the feasibility of Fe-MFC application in solar panel production wastewater treatment was discussed. The conclusions obtained are of great significance for solar panel production wastewater treatment and lay the foundation for the development of the photovoltaic industry.

2. Materials and Methods

2.1. The Characteristics of Actual Wastewater

The solar panel production wastewater was sampled from a solar panel production manufacturer in Yinchuan City, China. The raw wastewater was strongly acidic. Thus, the pH of the raw water was adjusted to 7 before the experiment. The main contents of the raw solar panel production wastewater are shown in Table 1.

Table 1. Contents of solar panel production wastewater.

Water Quality Index	Concentration	Water Quality Index	Concentration
NO_3^- -N	340.6 mg/L	pH	2.5
Ca^{2+}	103.8 mg/L	conductivity	4.9 ms/cm
Mg^{2+}	41.8 mg/L	turbidity	0 UNT
Na^{2+}	287.9 mg/L	COD	76.9 mg/L
K^+	18.7 mg/L	ORP	462 mV
NH_4^+ -N	95.6 mg/L	NO_2^- -N	45.0 mg/L

2.2. Construction of Microbial Fuel Cell

A two-chamber Fe-anode microbial fuel cell (Fe-MFC) (Figure 1) was used to treat the solar panel production wastewater. The Fe-MFC was made of first-class borosilicate glass, with an inner diameter of 3 cm. The total volume of Fe-MFC was 160 mL while the effective volume was 100 mL. A piece of iron sheet (from a waste iron recycling station in Xi'an) ($3\text{ cm} \times 6\text{ cm} \times 0.2\text{ mm}$) with high purity (99%) was used as the anode. A carbon fiber brush connected mainly by a titanium rod ($d = 3\text{ cm}$, $\varphi = 6\text{ cm}$) was used as the cathode. The carbon fiber brush was covered with denitrification biofilm. The cathode denitrifying biofilm was formed by the acclimation of denitrifying granular sludge by magnetic stirring. The acclimation time was 7 days, and obvious biofilm could be observed on the cathode carbon fiber brush. The distance between the anode and cathode was controlled at 6 cm, and the two chambers were separated by NaFion 117 proton exchange membrane (PEM, DuPont, Wilmington, USA) with 7.5 cm^2 . The anode and cathode were connected externally with titanium wire, and the external resistance was $1000\ \Omega$.

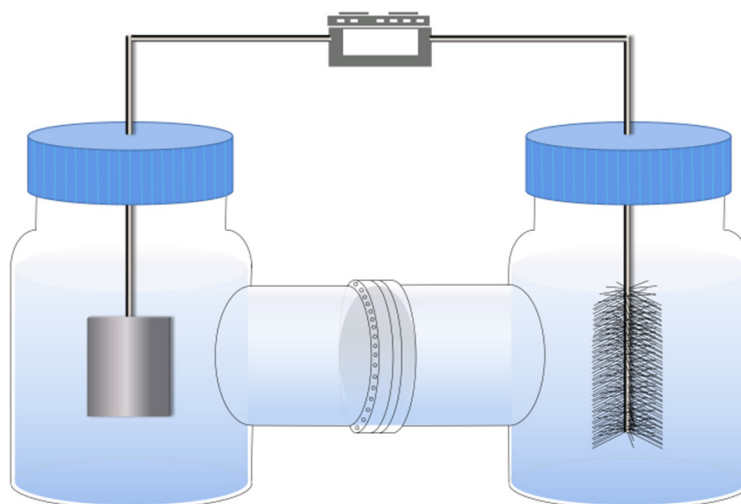


Figure 1. The setup of the two-chamber Fe-anode microbial fuel cell.

2.3. Experiments Design and Basic Analysis

The KH_2PO_4 solution with a concentration of 1088 mg/L was used as the anode electrolyte. The actual wastewater from the solar panel production manufacturer was used as the cathode liquid. After 30 min aeration by argon gas, the Fe-MFC was operated in the thermostat (Kewei, China) with a temperature of 30° . The HRT was set as 7 days according to the pre-experiment results. The Fe-MFC was operated in a sequencing batch for six cycles (100% feeding rates and 80% discharging rates for each cycle), for a total of 42 days.

At intervals, samples were taken out from the Fe-MFC to determine the NO_3^- -N and Fe^{2+} concentrations by an ultraviolet-visible spectrophotometer (Younike, China) according to the standard methods (Standard Methods for the Examination of Water and Wastewater, 2006). All wastewater samples were filtered by $0.45\ \mu\text{m}$ filtration membrane before concentration determination. The pH value was measured by a portable pH meter.

2.4. Denitrification Efficiency

According to Section 2.3, the initial and final concentrations of NH_4^+ -N, NO_3^- -N and NO_2^- -N in Fe-MFC were measured. The nitrate nitrogen volumetric loading (NLR) and nitrate nitrogen removal rate (NRR) in each cycle were calculated, and the change trends of NLR and NRR versus time were plotted.

The water samples were filtered by a $0.45\ \mu\text{m}$ water filter membrane before sample determination. The content of NH_4^+ -N was determined by Nessler's reagent spectrophotometry. The content of NO_3^- -N was determined by the phenol disulfonic acid spectrophotometric

method; the content of NO_2^- -N was determined by *N*-(1-naphthyl)-ethylenediamine spectrophotometry.

2.5. Electrochemical Efficiency

2.5.1. The Output Voltage and Conversion Efficiency

The instantaneous output voltage of the Fe-MFC was automatically recorded by a data acquisition board (USB_HRF105) every minute during the sequencing batch operation. Then the average value was calculated every 30 min and the output voltage below.

To assess the contribution of MFC to nitrate removal, the conversion efficiency (CE) of the bio-cathode was calculated by the following Equations (1) and (2).

$$\text{CE}(\%) = \Delta m_{\text{exp}} / \Delta m_{\text{theor}} \quad (1)$$

$$\Delta m_{\text{theor}} = \int IT/nF \quad (2)$$

where Δm_{exp} (mol) represents the amount of nitrate reduced within the experimental time T (s); Δm_{theor} (mol) is the quantity of nitrate that can be reduced theoretically by bio-cathode in Fe-MFC. I (A) represents the real-time current of the Fe-MFC; T (s) stands for reaction time; F (Faraday constant) is $96,485 \text{ C} \cdot \text{mol}^{-1}$; the n value is the number of electrons required to reduce/oxidize per mol substrate, where the n value of nitrate reduction to nitrogen gas is 5.

2.5.2. The Cyclic Voltammetry Method

The cyclic voltammetry method was used to measure and analyze the electrochemical efficiency of the bio-cathode in Fe-MFC. The cathode electrode, anode electrode and Ag/AgCl reference electrode were scanned and CV curves were drawn. The voltage sweep range of the CV curve was set from -0.4 V to 0.4 V , and the sweep speed was 5 mV/s . The graph which was obtained through the cyclic voltammetry curve at the last time was integrated, and then the integrated voltammetry electric charge per unit area of the electrode can be calculated by Equation (3) [29].

$$q^* = \frac{\int_{E_1}^{E_2} i(E) dE}{v} \quad (3)$$

where q^* represents the voltammetry electric charge, C/cm^2 ; E_1 and E_2 are the lower and upper limits of the CV scanning test, V ; $i(E)$ is the change function of electron current with scanning potential; v is the electric potential scanning rate, V/s .

2.5.3. Electrochemical Impedance Spectroscopy (EIS) Test

The internal resistance of the Fe-MFC reactor was measured and analyzed by the electrochemical impedance spectroscopy (EIS) test. The spectral characteristics were tested under steady-state conditions by applying a low voltage or current-interfering signal to the MFC [30]. The equivalent circuit diagram [31] was shown in Figure S1.

The Fe-MFC was replaced with fresh electrolyte and remained as a closed circuit for 2 h before the EIS test was conducted. During the EIS test, a three-electrode system with a frequency ranging from 100 KHz to 10 MHz was used to analyze the change of R_{ohm} and R_{ct} values by the Nyquist diagram, so as to analyze the influence on the denitrification process of the MFC reactor.

2.6. Microbial Community Analysis

In order to characterize the bacterial community in the denitrification biofilm covering the bio-cathode, the microbial genomic DNA was extracted using the DNA extraction kit (MP Biochemicals, California, USA); the purity and concentration of DNA were detected using Thermo NanoDrop One. Universal primers 338 F and 806R were synthesized by Invitrogen (Invitrogen, Carlsbad, CA, USA), containing $25 \mu\text{L} \times 2 \times$ Premix Taq (Takara

Biotechnology, Dalian Co., Ltd., Dalian, China), 1 μL each primer (10 μM) and 3 μL DNA (20 $\text{ng}/\mu\text{L}$) template in a volume of 50 μL , were used for PCR amplification of the 16S rRNA genes by thermocycling. The PCR amplification and gene sequencing were accomplished by Guangdong Magigene Biotechnology Co., Ltd. Guangzhou, China.

3. Results and Discussion

3.1. Denitrification Efficiency

The solar panel production wastewater was used as a catholyte of Fe-MFC and the Fe-MFC was continuously operated in sequencing batch for six cycles. The cathode provided electrons for denitrification directly. In fact, the electrons were originally from the iron anode [32,33]. The denitrification bacteria on the carbon brush reduced NO_3^- to N_2 achieving NO_3^- removal. As shown in Figure 2, the Fe-MFC showed a significant removal efficiency of NO_3^- . The maximum removal loading rate and removal efficiency of NO_3^- -N was $0.049 \text{ kg}\cdot\text{m}^{-3}\cdot\text{d}^{-1}$ and 99.98%. The maximum removal efficiency of NH_4^+ was 79.1%. However, both indexes decreased gradually along with the cycles to $0.024 \text{ kg}\cdot\text{m}^{-3}\cdot\text{d}^{-1}$ and 48.22% finally (Figure 2a). The total decrease in nitrate removal efficiency from cycle 1 to 6 was 48.22%, while for the first and last two cycles, the decrease was 3.09% and 21.41%, respectively. Based on the first-order reaction kinetic, the rate constant of autotrophic denitrification on the cathode in each cycle was calculated and shown in Table 2. The reaction rate constant decreased along with the cycle, and the reaction rate constant in cycle 1 was two times more than that in cycle 6. The sharp decrease in denitrification efficiency and denitrification rate in the last cycles was considered to be related to the passivation of the anode iron sheet and the loss of biomass on the bio-cathode [1,21,34].

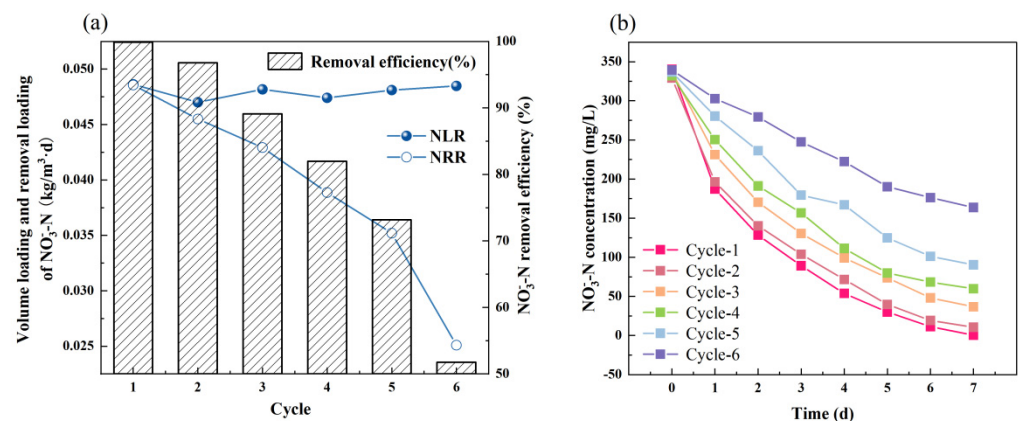


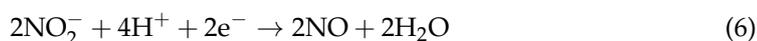
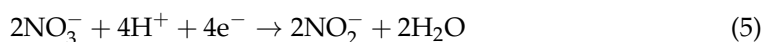
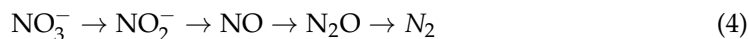
Figure 2. (a) The volumetric loading rate and removal efficiency of nitrate nitrogen in each cycle; (b) The nitrate nitrogen concentration curve with time in each cycle.

Table 2. The fitting of data in Figure 2b by the zero-order kinetics ($c_t - c_0 = -kt$).

Cycle	1	2	3	4	5	6
k	59.88 ± 5.70	55.36 ± 4.77	51.184 ± 3.89	46.54 ± 3.10	40.04 ± 1.88	27.53 ± 0.83
R ²	0.9318	0.94351	0.95568	0.96556	0.98259	0.99282

With the release of Fe^{2+} , the anode iron sheet became thinner and thinner, and even holes were formed on its surface [35,36]. Moreover, the exposed surface of the anode iron sheet was covered with amorphous white compounds, and it was considered that it may be phosphate-iron compounds (Wang et al., 2019), which intensifies the passivation of the anode. The passivation of the iron anode resulted in a decrease in the current and electron transfer efficiency [21]. Meanwhile, the denitrifying bacteria on the cathode gradually died due to the decrease in electron donors caused by passivation, followed by a decrease in the denitrification efficiency.

The NO_3^- was reduced to N_2 by multiple steps Equations (4)–(8). The accumulation of intermediate product nitrite (NO_2^-) during the denitrification process may have detrimental effects on the denitrifying bacteria and inhibit the denitrification efficiency [37,38]. However, during the running cycles of Fe-MFC, NO_2^- in the catholyte was barely detected, while the concentration of NH_4^+ -N was maintained at 20 mg/L, indicating most of NO_3^- was removed from the wastewater in the form of gas; however, it should be noted that gases such as $\text{NO}/\text{N}_2\text{O}$ may have a certain negative impact on the environment, and their release should be avoided as much as possible.



Compared with the treatment of simulated wastewater, the NO_3^- -N removal rate and efficiency by Fe-MFC to treat actual wastewater improved 10 times and 2 times, respectively [21,36]. The effluent concentration of NO_3^- -N met the emission requirement of solar panel production wastewater in China, endowing the Fe-MFC technology with broad application prospects.

3.2. Electrochemical Efficiency

Besides the pollutants removal, electricity was generated by the Fe-MFC as electrons were transported from the iron anode to the bio-cathode. The output voltages of Fe-MFC in six cycles were monitored and plotted in Figure 3a, and the conversion efficiencies of bio-cathode in each cycle were calculated and shown in Figure 3b.

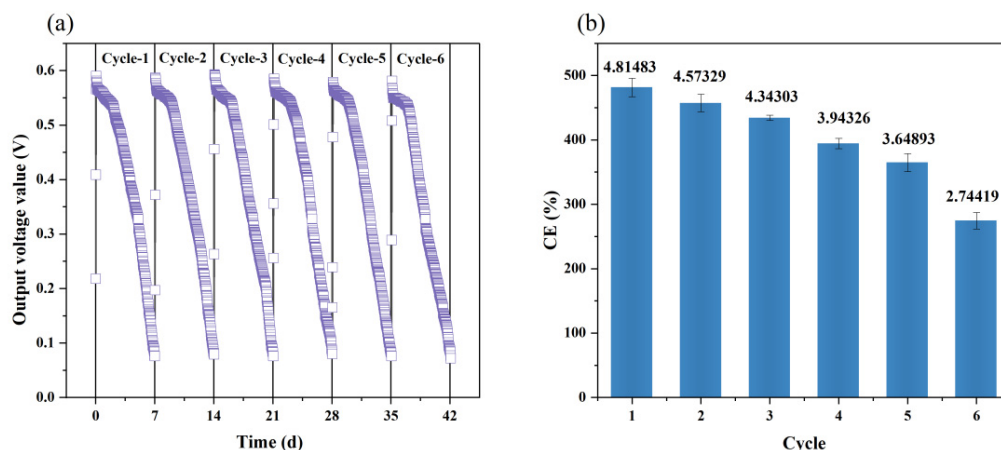


Figure 3. (a) The output voltage of Fe-MFC; (b) The conversion efficiency in each cycle.

In Figure 3a, the trend of output voltage along with time in each cycle was quite similar. At the beginning of each cycle, the output voltage was very close to the open circuit voltage due to the instantaneous connection of the circuit. The maximum output voltage (560 ± 10 mV) was achieved in two hours, and the value was quite higher than the reported ones (Wang et al., 2022b; Ghafari et al., 2008), indicating a big step for electricity production by bio-cathode denitrification MFC. Then the output voltage entered the plateau

(520 ± 50 mV) lasting around 40 h. The output voltage decreased all the way to the bottom as the substrate (NO_3^- -N) was depleted [1,17].

From cycle 1 to 6, the average output voltage of the plateau in six cycles gradually decreased, which may be caused by the biofilm aging [1]. As a result, the coulombic efficiency gradually decreased with time in Figure 3b. Kinds of factors may influence the coulombic efficiency, i.e., electrolyte decomposition, interface passivation, and changes of electrode active materials [24,39]. The reduction in coulomb efficiency in Figure 3b showed that the cathode biofilm gradually aged and the redox reaction of the system was inhibited along with time, resulting in a decrease in electrochemical activity [39].

In order to analyze the reversibility and polarization degree of the electrochemical reaction on the bio-cathode, the cyclic voltammetry method was used to measure the CV curves of the cathode during each cycle. The bio-cathode CV curves were all flat and without obvious redox peaks, indicating that the adsorption of cathode electric double layers to electric charge was the main storage method of electricity [40,41]. The CV curve of the classical ideal capacitor showed a symmetrical rectangular shape. The bio-cathode CV curve showed an obvious asymmetric rectangular shape, indicating that it was an irreversible oxidation-reduction reaction in Fe-MFC [26,41]. According to Figure S2b, the q^* value of the cathode decreased along with the operation time, indicating a decrease in the electrocatalytic activities of the bio-cathode. The deterioration of the bio-cathode was supposed to result in the aging of the biofilm and the decrease in the electron transfer efficiency [26]. This all led to the a decrease in the denitrification efficiency of Fe-MFC.

EIS is an electrochemical method to analyze the charge transfer and material diffusion of the electrode, indicating the variation trend of internal resistance and evaluating the denitrification process [42]. To further clarify the specific component of the cathode internal resistance, an EIS test was used and the results are shown in Figure 4 and Table 3. All of the ohmic resistance, charge transfer and activation resistance increased along with the operation time, indicating the decrease in the cathode electrical activity, which was speculated to be caused by the aging of biofilm on the bio-cathode [26,31].

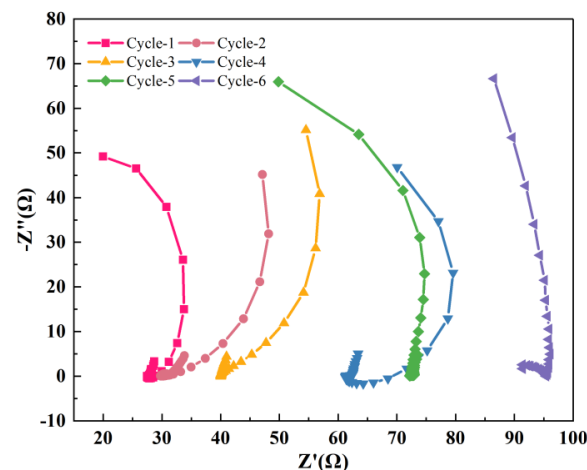


Figure 4. Nyquist curves of EIS tests in different cycles.

Table 3. Rohm and R_{ct} values in different cycles.

Cycle	1	2	3	4	5	6
R_{ohm} (Ω)	0.756	0.833	1.072	1.615	1.747	1.886
R_{ct} (Ω)	29.71	40.37	52.57	60.39	72.06	94.79

3.3. Microbial Community Analysis of Bio-Cathode Biofilm

The composition of the microbial community on the bio-cathode was related to the denitrification efficiency (Ovez et al., 2006; Luo, 2022). Therefore, 16S rRNA gene sequenc-

ing was performed on the biofilm at intervals. As shown in Table 4, the biodiversity indices, including operational classification units (OTUs), ACE, Chao 1, Shannon, and Simpson were listed. All indices showed that the biodiversity increased along with the operation time, then decreased. It is quite possible that it resulted from the adaption of microorganisms to the new environment, especially the electron donor for denitrification changed from chemicals to the cathode [28,32]. The coverage of all samples was greater than 0.999, indicating the accuracy of sequencing results [43].

Table 4. Numbers of the OTUs and biodiversity of cathode biofilm.

Sample	OUT-Num	ACE-Index	Chao1-Index	Coverage	Shannon-Index	Simpson
Day 1	378	419.24	378.2	0.99938	1.69	0.611
Day 7	486	525.27	486.1	0.99942	2.45	0.452
Day 28	546	581.01	546.1	0.99934	4.18	0.142
Day 42	509	536.07	509.1	0.99949	3.95	0.148

At the phylum level, no significant fluctuation in the microbial composition was observed during the whole operation time (Figure S3). *Proteobacteria* always predominated, but its proportion decreased from 91.43% to 51.43%. *Proteobacteria* had been reported as the predominant phylum in several electrochemical systems [44–46], as most bacteria of *Proteobacteria* could mediate electron transfer extracellularly [47]. Followed were *Firmicutes* and *Bacteroidetes*, the total abundance increased from 8.43% on day 1 to 45.55% on day 42. *Firmicutes* and *Bacteroidetes* were reported to be involved in the degradation of complex pollutants and microbial electricity generation in MFC [47–49].

At the genus level, *Acinetobacter* (77.70%) was dominant in the early time, soon afterward *Chryseobacterium* (31.21%), *Thermomonas* (22.99%), and *Thauera* (12.55%) became the dominant genus gradually (Figure 5). *Unassigned-Rhodobacteraceae* (19.38%) also increased. *Acinetobacter* showed remarkable denitrification ability [50,51], and they could utilize coenzymes [44,52]. The proportion of *Acinetobacter* in bio-cathode biofilm gradually decreased, probably because they were difficult to adapt to the environment with cathode as direct electron donors. *Chryseobacterium* and *Thermomonas* were reported generally to be enriched on bio-cathodes and they could use nitrate as an electron acceptor for metabolism [53,54]. As the typical denitrification genus of *Proteobacteria*, *Thauera* could reduce NO_3^- -N with the cathode as an electron donor [33]. Therefore, along with the operation time of Fe-MFC, *Chryseobacterium*, *Thermomonas*, and *Thauera* were enriched on bio-cathode under the autotrophic substrate environment. Other autotrophic microorganisms, such as *Brevundimonas* and *Petrimonas* [53,55,56], also bloomed along with time. The Fe-MFC offered a favorable living environment for autotrophic bacteria, thus the abundance of most genera showed obvious change.

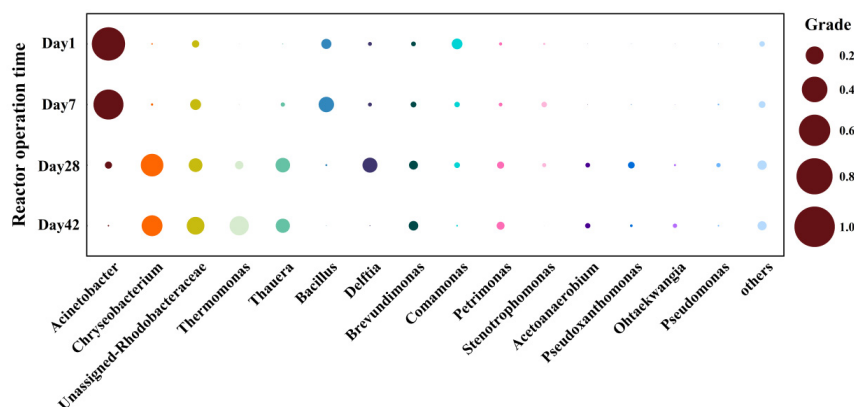


Figure 5. Relative abundance of different genera on cathodes on day 1, 7, 28 and day 42. (The area of bubble was positively correlated with relative abundance; genera accounting for <1% of total sequences were classified in the group ‘Others’).

In summary, *Proteobacteria* predominated in the microbial community on bio-cathode. When the electron donor changed from chemicals to the cathode, the abundance of *Acinetobacter* decreased sharply, while the amount of *Chryseobacterium*, *Thermomonas* and *Thauera* increased obviously as the latter ones could use the electrons from the cathode to reduce nitrate. Microorganisms that cannot adapt to the autotrophic environment in Fe-MFC died out finally, resulting in microbial succession in the cathode biofilm.

4. Conclusions

The two-chamber MFC with iron sheet as anode and denitrification biofilm as cathode showed remarkable NO_3^- removal efficiency when treating solar panel production wastewater. The NO_3^- -N removal efficiency reached a 99.98% maximum, and the corresponding removal loading rate was $0.049 \text{ kg}\cdot\text{m}^{-3}\cdot\text{d}^{-1}$. The output voltages rose rapidly to $560 \pm 10 \text{ mV}$ within 2 h and then stabilized at $520 \pm 50 \text{ mV}$ for about 40 h. Combining the detection of coulombic efficiency, CV curve, q^* value and internal resistance, the decrease in denitrification efficiency and electricity generation efficiency probably resulted from the passivation of the iron anode; the aging of cathode biofilm resulted in the efficiency decrease. The two-chamber MFC showed good denitrification efficiency and electricity generation efficiency when treating solar panel production wastewater. The Fe-MFC technology decreased the construction cost and operation cost for industrial wastewater treatment (Table S1), laying the foundation for the development of the photovoltaic industry. However, the further improvement of nitrate removal efficiency and the extension of electrode service life are still challenges that bio-cathode denitrification technology will face in the future.

Supplementary Materials: The following supporting information can be downloaded at: <https://www.mdpi.com/article/10.3390/w15193347/s1>.

Author Contributions: Conceptualization, R.W.; Data curation, L.C.; Investigation, L.C.; Methodology, J.L. and L.L.; Resources, L.Y. and R.W.; Supervision, R.W.; Validation, L.C.; Visualization, L.C. and B.L.; Writing—original draft, C.D.; Writing—review and editing, L.C. All authors have read and agreed to the published version of the manuscript.

Funding: This research was funded by [National Natural Science Foundation of China] grant number [51808433, 51878538] and [Shaanxi Provincial Education Department Youth Innovation team research project] grant number [22]P036].

Data Availability Statement: <http://cloud.magigene.com/>.

Conflicts of Interest: The authors declare no conflict of interest.

References

1. Fang, S.B.; Zhang, J.X.; Niu, Y.F.; Ju, S.H.; Gu, Y.W.; Han, K.; Wan, X.X.; Li, N.; Zhou, Y. Removal of nitrate nitrogen from wastewater by green synthetic hydrophilic activated carbon supported sulfide modified nanoscale zerovalent Iron: Characterization, performance and mechanism. *Chem. Eng. J.* **2023**, *461*, 141990. [CrossRef]
2. Hui, K.L.; Yuan, Y.; Xi, B.D.; Tan, W.B. A review of the factors affecting the emission of the ozone chemical precursors VOCs and NOx from the soil. *Environ. Int.* **2023**, *172*, 107799. [CrossRef] [PubMed]
3. Egrinya Eneji, A.; Islam, R.; An, P.; Amalu, U.C. Nitrate retention and physiological adjustment of maize to soil amendment with superabsorbent polymers. *J. Clean. Prod.* **2013**, *52*, 474–480. [CrossRef]
4. Kassaei, M.; Motamedi, E.; Mikhak, A.; Rahnemaie, R. Nitrate removal from water using iron nanoparticles produced by arc discharge vs. reduction. *Chem. Eng. J.* **2011**, *166*, 490–495. [CrossRef]
5. Meng, S.; Ling, Y.; Yang, M.Y.; Zhao, X.G.; Osman, A.I.; Al-Muhtaseb, A.H.; Rooney, D.W.; Yap, P.S. Recent research progress of electrocatalytic reduction technology for nitrate wastewater: A review. *J. Environ. Chem. Eng.* **2023**, *11*, 109418. [CrossRef]
6. Zou, X.Y.; Chen, C.J.; Wang, C.H.; Zhang, Q.; Yu, Z.W.; Wu, H.P.; Zhuo, C.; Zhang, T.C. Combining electrochemical nitrate reduction and anammox for treatment of nitrate-rich wastewater: A short review. *Sci. Total Environ.* **2021**, *800*, 149645. [CrossRef] [PubMed]
7. Ghafari, S.; Hasan, M.; Aroua, M.K. Bio-electrochemical removal of nitrate from water and wastewater—A review. *Bioresour. Technol.* **2008**, *99*, 3965–3974. [CrossRef]

8. Zhang, H.; Li, H.F.; Gao, D.D.; Yu, H.R. Source identification of surface water pollution using multivariate statistics combined with physicochemical and socioeconomic parameters. *Sci. Total Environ.* **2021**, *806*, 12. [[CrossRef](#)]
9. Mohajeri, P.; Smith, C.M.S.; Chau, H.W.; Lehto, N. ALLODUST augmented activated sludge single batch anaerobic reactor (AS-SBAnR) for high concentration nitrate removal from agricultural wastewater. *Sci. Total Environ.* **2021**, *752*, 141905. [[CrossRef](#)]
10. Wu, Y. Treatment process design of the wastewater from the production of silicon solar panels. *Ind. Water Treat.* **2021**, *41*, 138–142. [[CrossRef](#)]
11. Shi, P.; Zhang, Y.; Song, J.; Li, P.; Wang, Y.-S.; Zhang, X.; Li, Z.-B.; Bi, Z.; Zhang, X.; Qin, Y.-L.; et al. Response of nitrogen pollution in surface water to land use and social-economic factors in the Weihe River watershed, northwest China. *Sust. Cities Soc.* **2019**, *50*, 9. [[CrossRef](#)]
12. Kabuba, J.; Lephallo, J.; Rutto, H. Comparison of various technologies used to eliminate nitrogen from wastewater: A review. *J. Water Process Eng.* **2022**, *48*, 102885. [[CrossRef](#)]
13. Moloantoa, K.M.; Khetsha, Z.P.; Van Heerden, E.; Castillo, J.C.; Cason, E.D. Nitrate Water Contamination from Industrial Activities and Complete Denitrification as a Remediation Option. *Water* **2022**, *14*, 799. [[CrossRef](#)]
14. Zhou, X.L.; Bi, X.J.; Fan, X.; Yang, T.; Wang, X.D.; Chen, S.S.; Cheng, L.H.; Zhang, Y.; Zhao, W.H.; Zhao, F.C.; et al. Performance and bacterial community analysis of a two-stage A/O-MBBR system with multiple chambers for biological nitrogen removal. *Chemosphere* **2022**, *303*, 135195. [[CrossRef](#)]
15. Moghaddam, R.; Torres-Rojas, D.; Schipper, L. Enhanced nitrate removal and side effects of methanol dosing in denitrifying bioreactors. *Ecol. Eng.* **2022**, *185*, 106818. [[CrossRef](#)]
16. Chen, L.; Zhang, W.M.; Shen, Y.J.; Zhou, B. Practical operation of solar battery wastewater treatment plant. *Ind. Water Treat.* **2022**, *42*, 168–172. [[CrossRef](#)]
17. Chung, J.; Amin, K.; Kim, S.; Yoon, S.; Kwon, K.; Bae, W. Autotrophic denitrification of nitrate and nitrite using thiosulfate as an electron donor. *Water Res.* **2014**, *58*, 169–178. [[CrossRef](#)]
18. Rezvani, F.; Sarrafzadeh, M.H.; Ebrahimi, S.; Oh, H.M. Nitrate removal from drinking water with a focus on biological methods: A review. *Environ. Sci. Pollut. Res.* **2019**, *26*, 1124–1141. [[CrossRef](#)]
19. Saran, H.; Purchase, D.; Saratale, G.D.; Saratale, R.G.; Romanholo Ferreira, L.F.; Bilal, M.; Iqbal, H.M.N.; Hussain, C.M.; Mulla, S.I.; Bharagava, R.N. Microbial fuel cell: A green eco-friendly agent for tannery wastewater treatment and simultaneous bioelectricity/power generation. *Chemosphere* **2023**, *312*, 137072. [[CrossRef](#)]
20. Wang, S.F.; Liu, B.Y.; Tan, G.T.; Wang, R.; Yuan, L.J. Parameters' optimization of autotrophic denitrification on bio-cathode with iron as anode. *Acta Sci. Circumstantiae* **2022**, *42*, 137–145. [[CrossRef](#)]
21. Clauwaert, P.; Aelterman, P.; Pham, T.H.; De Schamphelaire, L.; Carballa, M.; Rabaey, K.; Verstraete, W. Minimizing losses in bio-electrochemical systems: The road to applications. *Appl. Microbiol. Biotechnol.* **2008**, *79*, 901–913. [[CrossRef](#)]
22. Wu, D.; Yi, X.; Tang, R.; Feng, C.; Wei, C. Single microbial fuel cell reactor for coking wastewater treatment: Simultaneous carbon and nitrogen removal with zero alkaline consumption. *Sci. Total Environ.* **2018**, *621*, 497–506. [[CrossRef](#)]
23. Virdis, B.; Rabaey, K.; Yuan, Z.; Keller, J. Microbial fuel cells for simultaneous carbon and nitrogen removal. *Water Res.* **2008**, *42*, 3013–3024. [[CrossRef](#)]
24. Xie, B.; Dong, W.; Liu, B.; Liu, H. Enhancement of pollutants removal from real sewage by embedding microbial fuel cell in anaerobic-anoxic-oxic wastewater treatment process. *J. Chem. Technol. Biotechnol.* **2014**, *89*, 448–454. [[CrossRef](#)]
25. Xie, B.; Liu, B.; Yi, Y.; Yang, L.; Liang, D.; Zhu, Y.; Liu, H. Microbiological Mechanism of the Improved Nitrogen and Phosphorus Removal by Embedding Microbial Fuel Cell in Anaerobic-Anoxic-Oxic Wastewater Treatment Process. *Bioresour. Technol.* **2016**, *207*, 109–117. [[CrossRef](#)]
26. Ding, A.Q.; Zhao, D.; Ding, F.; Du, S.W.; Lu, H.J.; Zhang, M.; Zheng, P. Effect of inocula on performance of bio-cathode denitrification and its microbial mechanism. *Chem. Eng. J.* **2018**, *343*, 399–407. [[CrossRef](#)]
27. Wang, H.; Wang, Q.; Li, X.; Wang, Y.; Jin, P.; Zheng, Y.; Huang, J.; Li, Q. Bioelectricity generation from the decolorization of reactive blue 19 by using microbial fuel cell. *J. Environ. Manag.* **2019**, *248*, 109310. [[CrossRef](#)]
28. Li, Z.H.; Zhang, Q.H.; Jiang, Q.R.; Zhan, G.Q.; Li, D.P. The enhancement of iron fuel cell on bio-cathode denitrification and its mechanism as well as the microbial community analysis of bio-cathode. *Bioresour. Technol.* **2019**, *274*, 1–8. [[CrossRef](#)]
29. Zhou, J.; Guan, W.X.; Wang, S.F.; Zhang, X.M. Electrochemical active surface area of Ti/IrO₂+MnO₂ electrodes in the acid solutions. *Chem. Ind. Eng. Prog.* **2019**, *38*, 3782–3787. [[CrossRef](#)]
30. Shi, X.X. Research on cathodic structure and catalyst of air-cathode microbial fuel cells. *Harbin Inst. Technol.* **2013**. [[CrossRef](#)]
31. Wagner, N. Characterization of membrane electrode assemblies in polymer electrolyte fuel cells using a.c. impedance spectroscopy. *J. Appl. Electrochem.* **2002**, *32*, 859–863. [[CrossRef](#)]
32. Li, X.; Wang, X.; Zhang, Y.; Zhao, Q.; Yu, B.; Li, Y.; Zhou, Q. Salinity and conductivity amendment of soil enhanced the bioelectrochemical degradation of petroleum hydrocarbons. *Sci. Rep.* **2016**, *6*, 32861. [[CrossRef](#)]
33. Xiao, Y.; Zheng, Y.; Wu, S.; Yang, Z.H.; Zhao, F. Bacterial community structure of autotrophic denitrification biocathode by 454 pyrosequencing of the 16S rRNA gene. *Microb. Ecol.* **2015**, *69*, 492–499. [[CrossRef](#)]
34. Xu, L.; Zhao, Y.Q.; Doherty, L.; Hu, Y.S.; Hao, X.D. Promoting the bio-cathode formation of a constructed wetland-microbial fuel cell by using powder activated carbon modified alum sludge in anode chamber. *Sci. Rep.* **2016**, *6*, 26514. [[CrossRef](#)] [[PubMed](#)]

35. Gao, C.Q.; Yu, W.; Zhu, Y.C.; Wang, M.; Tang, Z.Z.; Du, L.; Hu, M.Y.; Fang, L.; Xiao, X.C. Preparation of porous silicate supported micro-nano zero-valent iron from copper slag and used as persulfate activator for removing organic contaminants. *Sci. Total Environ.* **2021**, *754*, 142131. [[CrossRef](#)]
36. Liu, Y.; Wang, J.L. Reduction of nitrate by zero valent iron (ZVI)-based materials: A review. *Sci. Total Environ.* **2019**, *671*, 388–403. [[CrossRef](#)] [[PubMed](#)]
37. Li, W.; Shan, X.Y.; Wang, Z.Y.; Lin, X.Y.; Li, X.C.; Cai, C.Y.; Abbas, G.; Zhang, M.; Shen, L.D.; Hu, Z.Q.; et al. Effect of self-alkalization on nitrite accumulation in a high-rate denitrification system: Performance, microflora and enzymatic activities. *Water Res.* **2016**, *88*, 758–765. [[CrossRef](#)]
38. Deng, S.H.; Peng, S.; Ngo, H.H.; Jin-An Oh, S.; Hu, Z.F.; Yao, H.; Li, D.S. Characterization of nitrous oxide and nitrite accumulation during iron (Fe(0))- and ferrous iron (Fe(II))-driven autotrophic denitrification: Mechanisms, environmental impact factors and molecular microbial characterization. *Chem. Eng. J.* **2022**, *438*, 135627. [[CrossRef](#)]
39. Freguia, S.; Rabaey, K.; Yuan, Z.; Keller, J. Electron and carbon balances in microbial fuel cells reveal temporary bacterial storage behavior during electricity generation. *Environ. Sci. Technol.* **2007**, *41*, 2915–2921. [[CrossRef](#)] [[PubMed](#)]
40. Xia, X.; Tokash, J.C.; Zhang, F.; Liang, P.; Huang, X.; Logan, B.E. Oxygen-reducing biocathodes operating with passive oxygen transfer in microbial fuel cells. *Environ. Sci. Technol.* **2013**, *47*, 2085–2091. [[CrossRef](#)]
41. Endut, Z.; Hamdi, M.; Basirun, W.J. An investigation on formation and electrochemical capacitance of anodized titania nanotubes. *Appl. Surf. Sci.* **2013**, *280*, 962–996. [[CrossRef](#)]
42. Yin, Y.; Huang, G.; Chen, J.; Liu, Y. Electrochemical Behavior of Microbial Fuel Cell in a Start-up Phase. *J. East. China Univ. Sci. Technol. Nat. Sci. Ed.* **2014**, *40*, 190–195. [[CrossRef](#)]
43. Wang, Y.; Chen, Y.; Wen, Q.; Zheng, H.; Xu, H.; Qi, L. Electricity generation, energy storage, and microbial-community analysis in microbial fuel cells with multilayer capacitive anodes. *Energy* **2019**, *189*, 116342. [[CrossRef](#)]
44. Chang, C.C.; Kao, W.; Yu, C.P. Assessment of voltage reversal effects in the serially connected biocathode-based microbial fuel cells through treatment performance, electrochemical and microbial community analysis. *Chem. Eng. J.* **2020**, *397*, 125368. [[CrossRef](#)]
45. Krishna, K.V.; Mohan, S.V. Selective enrichment of electrogenic bacteria for fuel cell application: Enumerating microbial dynamics using MiSeq platform. *Bioresour. Technol.* **2016**, *213*, 146–154. [[CrossRef](#)]
46. Xu, X.; Zhao, Q.L.; Wu, M.S.; Ding, J.; Zhang, W.X. Biodegradation of organic matter and anodic microbial communities analysis in sediment microbial fuel cells with/without Fe(III) oxide addition. *Bioresour. Technol.* **2017**, *225*, 402–408. [[CrossRef](#)]
47. Schilirò, T.; Tommasi, T.; Armato, C.; Hidalgo, D.; Traversi, D.; Bocchini, S.; Gilli, G.; Pirri, C.F. The study of electrochemically active planktonic microbes in microbial fuel cells in relation to different carbon-based anode materials. *Energy* **2016**, *106*, 277–284. [[CrossRef](#)]
48. Chen, P.; Jiang, J.W.; Zhang, S.X.; Wang, X.Y.; Guo, X.Y.; Li, F.X. Enzymatic response and antibiotic resistance gene regulation by microbial fuel cells to resist sulfamethoxazole. *Chemosphere* **2023**, *325*, 138410. [[CrossRef](#)]
49. Zhao, C.F.; Liu, B.; Meng, S.Y.; Wang, Y.H.; Yan, L.J.; Zhang, X.W.; Wei, D. Microbial fuel cell enhanced pollutants removal in a solid-phase biological denitrification reactor: System performance, bioelectricity generation and microbial community analysis. *Bioresour. Technol.* **2021**, *341*, 125909. [[CrossRef](#)]
50. Ali, A.; Wu, Z.Z.; Li, M.; Su, J.F. Carbon to nitrogen ratios influence the removal performance of calcium, fluoride, and nitrate by *Acinetobacter* H12 in a quartz sand-filled biofilm reactor. *Bioresour. Technol.* **2021**, *333*, 125154. [[CrossRef](#)]
51. Su, J.F.; Zheng, S.C.; Huang, T.L.; Ma, F.; Shao, S.C.; Yang, S.F.; Zhang, L.N. Characterization of the anaerobic denitrification bacterium *Acinetobacter* sp. SZ28 and its application for groundwater treatment. *Bioresour. Technol.* **2015**, *192*, 654–659. [[CrossRef](#)] [[PubMed](#)]
52. Liu, H.; Matsuda, S.; Hashimoto, K.; Nakanishi, S. Flavins secreted by bacterial cells of *Shewanella* catalyze cathodic oxygen reduction. *ChemSusChem* **2012**, *5*, 1054–1058. [[CrossRef](#)] [[PubMed](#)]
53. Chen, F.; Li, Z.L.; Ye, Y.; Lv, M.; Liang, B.; Yuan, Y.; Cheng, H.Y.; Liu, Y.; He, Z.W.; Wang, H.C.; et al. Coupled sulfur and electrode-driven autotrophic denitrification for significantly enhanced nitrate removal. *Water Res.* **2022**, *220*, 118675. [[CrossRef](#)] [[PubMed](#)]
54. Park, H.I.; Kim, J.S.; Kim, D.K.; Choi, Y.J.; Pak, D. Nitrate-reducing bacterial community in a biofilm-electrode reactor. *Enzym. Microb. Technol.* **2006**, *39*, 453–458. [[CrossRef](#)]
55. Khanongnuch, R.; Di Capua, F.; Lakaniemi, A.M.; Rene, E.R.; Lens, P.N. H₂S removal and microbial community composition in an anoxic biotrickling filter under autotrophic and mixotrophic conditions. *J. Hazard. Mater.* **2019**, *367*, 397–406. [[CrossRef](#)]
56. Burgmann, H.; Jenni, S.; Vazquez, F.; Udert, K.M. Regime shift and microbial dynamics in a sequencing batch reactor for nitrification and anammox treatment of urine. *Appl. Environ. Microbiol.* **2011**, *77*, 5897–5907. [[CrossRef](#)]

Disclaimer/Publisher's Note: The statements, opinions and data contained in all publications are solely those of the individual author(s) and contributor(s) and not of MDPI and/or the editor(s). MDPI and/or the editor(s) disclaim responsibility for any injury to people or property resulting from any ideas, methods, instructions or products referred to in the content.